Fluorescence Study of the Coil-Globule Transition of a PEO Chain in Toluene

J. P. S. Farinha,† Susana Piçarra, K. Miesel, and J. M. G. Martinho*,‡

Centro de Química-Física Molecular, Instituto Superior Técnico, 1049-001 Lisboa, Portugal

Received: April 18, 2001; In Final Form: August 8, 2001

The cyclization kinetics of a poly(ethylene oxide) (PEO) chain ($M_n = 3280$; $M_w/M_n = 1.05$) labeled at both ends with pyrene was studied in toluene at several temperatures. Above 30 °C, the kinetics of pyrene excimer formation is well described by a two-state model. Below this temperature, a new excited species appears, which we identified as being a pyrene dimer. The appearance of the pyrene dimer was associated with a broad coil−globule transition. For lower temperatures, the kinetics of pyrene excimer and dimer formation can only be described by a three-states model. The fluorescence decay curves of the polymer in toluene were analyzed according to these models in order to obtain the rate constants. The activation energies of the cyclization and ring-opening processes were obtained from the Arrhenius plots of the rate constants. The activation energies for the cyclization processes (excimer and excited dimer formation) are close to the viscous flow activation energies. From the excimer dissociation rate constants, we calculated the binding energies of the excimer (36 ± 4 kJ mol^{-1} in the coil and 33 ± 1 kJ mol^{-1} in the globule) and the dimer (22 ± 2 kJ mol^{-1}). The van t'Hoff plots of the corresponding equilibrium constants allowed us to calculate the enthalpy and entropy of cyclization. The entropy values are negative according to a loss of entropy upon chain cyclization. The difference between the enthalpy and the binding energy of the excimer in both the globule and coil sates reflects the variation of polymer conformations between the cyclized and noncyclized chains.

Introduction

The study of the transition between the coil and globule conformations can have a significant contribution to our understanding of the polymer segment−segment and segment−solvent interactions. It also plays an important role in biology, enzymatic activity and protein folding,[1,2] DNA packing,[3] etc.

The conformation of a polymer chain in solution depends on both the polymer (composition and structure) and the solvent.[4,5] In a good solvent and for high molecular weight polymers, the chain adopts an extended coil conformation, owing to the exclude volume effect. In a θ solvent, the chains have unperturbed dimensions due to the balance between segment−segment and segment−solvent interactions. In a very poor solvent, the predominance of attractive segment−segment over segment−solvent interactions forces the polymer to collapse to the globular state.[4] The coil−globule transition can be induced by a change in the solvent thermodynamic condition or, equivalently, by lowering the temperature of the polymer solution below its θ_u point.[6] This change in conformation can take place as a sharp transition for long stiff polymer chains or as a broad transition for short flexible chains. These limits have been theoretically predicted and shown by simulation.[4,7,8]

Experimentally, the stable globule state of isolated chains is very difficult to approach without any aggregation and precipitation of the solute in the poor solvent. One has to work at extremely low concentrations, where most techniques (e.g. light scattering) are not sensitive enough. Here, we propose to use fluorescence to study the isolated chains in solution and detect the coil−globule transition. Fluorescence has been widely used to follow the dynamics and conformation of polymer chains in solution.[9−13] In these kinds of experiments, polymers have to be labeled with adequate chromophores, either along the main chain,[9,14] on a side-chain,[15] or at the chain ends.[10−16] Fluorescence anisotropy measurements of polymers labeled at the main chain[9,14] and at chain ends[16] give relevant information on the local motion (segmental motion) of the polymer chain. Namely, it was found that for a linear polymer in solution, the mobility of the chain ends is higher than that of the rest of the chain.[16] Fluorescence spectra and decay curves of side-chain fluorescent labeled polymers can give information on the conformation and dynamics of the chain as a whole. In this respect, Förster-type energy transfer[17] between fluorescent groups (one donor and one acceptor) attached at specific sites has been used as a spectroscopic ruler to calculate distances between labeled sites in synthetic polymers[18,19] and biopolymers.[20−23] The interchromophore distance should remain constant during the energy transfer process; otherwise, the measured distances would also reflect the motion of the polymer chain. In that case, fluorescence decays contain relevant information on the dynamics of the chain during the donor lifetime.[22,23]

Another strategy, pioneered by the work of Cuniberti and Perico,[24] was based on the fact that some electronically excited molecules can form an excited dimer (the excimer) on the encounter with a ground-state molecule. Following the time evolution of the excimer and monomer fluorescence of polymer chains labeled at both ends with an adequate fluorophore, it is possible to calculate the cyclization and ring-opening rate constants for the chain.[10−12] These rate constants provide information on both the initial conformation of the chain and its dynamics. The times involved on polymer cyclization are on the order of 10 ns to hundreds of nanoseconds, while the local motions measured by fluorescence anisotropy are in the nanoseconds or sub-nanoseconds time range. Cyclization studies report on the motion of the chain as a whole, which is evidenced

* To whom correspondence should be addressed.
† E-mail: farinha@ist.utl.pt.
‡ E-mail: jgmartinho@ist.utl.pt.

10.1021/jp011467e CCC: $20.00
Published on Web 10/03/2001

SCHEME 1

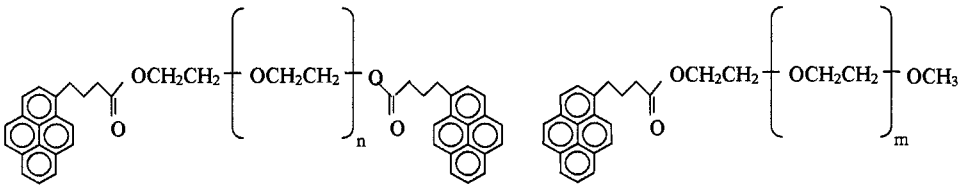

Polymer I **Polymer II**

by the direct dependence of the cyclization rate constant on the chain center of mass diffusion coefficient.[25] To access the dynamics of long chains, the polymers were labeled with long-lived fluorophores. In this respect, pyrene labeled chains were successfully used to study the influence of chain length,[26,27] solvent quality,[28−30] temperature,[27,31] and hydrostatic pressure.[32,33] These works were carried out in conditions where the chains adopt a coil conformation more or less expanded depending on the characteristics of the solvent and the polymer.

This paper describes the cyclization of a poly(ethylene oxide) (PEO), chain ($M_n = 3280$; $M_w/M_n = 1.05$) in toluene between −60 and 60 °C. The excimer to monomer fluorescence intensity ratio is practically constant from 60 to 30 °C, decreasing for lower temperatures. Above 30 °C, polymer cyclization is well described by a two-state (excited monomer and excimer) kinetic model. Fitting the pyrene monomer and excimer decay curves, one can calculate the cyclization and ring-opening rate constants at several temperatures. The cyclization is diffusion-controlled, with an activation energy similar to the solvent viscous flow activation energy. The excimer binding energy calculated from the Arrhenius plot of the dissociation rate constant has a value of 36 kJ mol^{-1}, similar to the value found for the intermolecular pyrene excimer.[34,35]

Below 20 °C, a three-state model is necessary to describe the decay curves of both pyrene monomer and excimer. This indicates the presence of a new excited species that was identified as a pyrene dimer. Indeed, the dimer is formed in the ground state as shown by the comparison of the excitation spectra measured at several wavelengths in the monomer and excimer emission regions. Dimers were not observed in toluene solutions at the same temperatures, neither for free pyrene nor for polystyrene chains of the same length, labeled with pyrene at both ends. The existence of pyrene dimers in the PEO solution in toluene is therefore induced by the polymer chain globular conformation below 30 °C.

From the analysis of the fluorescence decay curves, we calculate the rate constants for pyrene dimer and excimer formation and for the corresponding dissociation processes. The excimer and dimer formation rate constants are diffusion-controlled, with activation energies very close to the solvent viscous flow activation energy, showing that the globules are swollen by the solvent. Loose, solvent swollen globules were also observed in other polymeric systems, especially for flexible chains with molecular weights below the critical molecular weight M_e.[36] From the binding energies calculated for the dissociation processes in the coil and the globule, we show that the excimer do not reach the most stable configuration in the globule, probably due to constrains imposed by the "condensed" polymer chain. The low binding energy of the dimer explains the fast conversion of the excited dimer to excimer.

Experimental Section

Instrumentation. Fluorescence spectra were recorded on a SPEX Fluorolog F112A fluorimeter at several temperatures using a cryostat from Oxford Instruments (DN 1704) that allows the control of the temperature within ±0.5 °C. The fluorescence spectra were recorded between 370 and 600 nm using 345 nm as the excitation wavelength.

Time-resolved picosecond fluorescence intensity decays were obtained by the single-photon timing technique. The system consists of a mode-locked Coherent Inova 440-10 argon ion laser that synchronously pumped a cavity-dumped Coherent 701-2 DCM dye laser, delivering 5−6 ps pulses at a repetition rate of 460 kHz. The sample is electronically excited by vertically polarized light from the output of the DCM dye laser at the wavelength of 330 nm. The fluorescence was observed with a polarizer set at the magic angle, and the scattered light was eliminated by a cutoff filter. The emission, after being depolarized, passed through a Jobin-Yvon HR320 monochromator with a 100 lines/mm grating. The fluorescence of pyrene monomer (376 nm) and excimer (480 nm) was detected by a Hamamatsu 2809U-01 microchannel plate photomultiplier. Decay curve analysis was performed by a nonlinear least-squares method based on the Marquard algorithm.[37]

Polymer Synthesis and Materials. A poly(ethylene oxide) chain with OH terminal groups and average molecular weight of ca. 3400 g mol^{-1} and a poly(ethylene oxide) methyl ester chain with only one OH end group and molecular weight of ca. 5000 g mol^{-1} were purchased from Aldrich and purified by recrystallization in methanol. 1-Pyrenebutyric acid was obtained from Aldrich (97% purity) and used with no further purification. Toluene (99.57%), from Riedel-de-Haën, was carefully dried over sodium during several days. Pyridine was dried over KOH before being fractionated. The synthesis procedure was described elsewhere.[38] Activated charcoal and silica gel were added at the end of the reaction in order to remove colored impurities and nonreacted 4-(1-pyrenil)butyril choride.[39] The polymers were precipitated into cold methanol and further purified by gel permeation chromatography (GPC), using a Shephadex LH20 gel preparative column and methanol as eluent.[40] We obtained polymer **I**, labeled with pyrene at both chain ends and polymer **II**, labeled with pyrene at only one chain end (Scheme 1).

Polymer Characterization. From the ^{1}H NMR of polymer **I** in $CDCl_2CDCl_2$ (recorded in a 300 MHz Varian spectrometer), a degree of polymerization of 56 was calculated which corresponds to a molecular weight of 3130. This value agrees very well with the molecular weight ($M_n = 3280$) obtained by GPC using PEO standards and THF as eluent. The polymer has a very narrow molecular weight distribution ($M_w/M_n = 1.05$). Polymer **II** was characterized by GPC, with $M_n = 4600$ ($M_w/M_n = 1.05$). The degree of labeling of polymer **I** was determined by UV−vis absorption in toluene using for the molar absorption coefficient of the pyrene terminated chain the 1-pyrenebutyric acid value. A degree of labeling of 2.08 was obtained, showing that within experimental error both ends of the polymer chain are pyrene labeled.

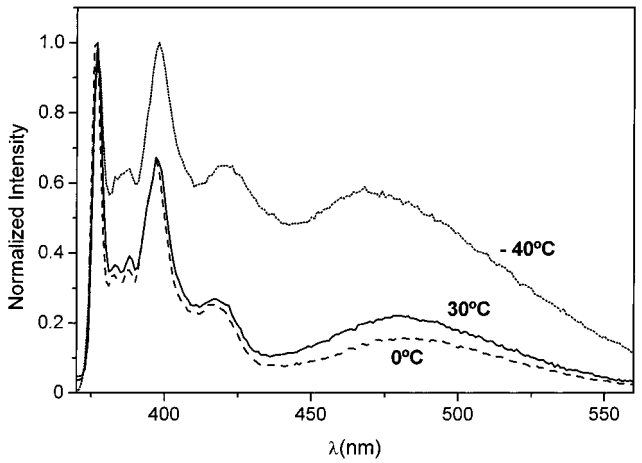

Figure 1. Normalized fluorescence spectra of a poly(ethylenoglicol) chain ($M_n = 3280$; $M_w/M_n = 1.05$), both ends labeled with pyrene, in tolune (10^{-6} M) at several temperatures: (−) 30, (- - -) 0, and (···) −40 °C.

Sample Preparation. The polymer **I** and polymer **II** dilute solutions (1.0×10^{-6} M) were prepared in spectragrade toluene. The solutions were degassed by the freeze−pump−thaw technique (6 cycles) and sealed, the final pressure being better than 10^{-5} bar. The solutions were kept in the dark at room temperature between measurements.

Results and Discussion

Steady-State Measurements. The room-temperature fluorescence spectrum of a diluted solution (10^{-6} M) of polymer **I** in toluene shows two separate emission bands: the characteristic structured emission of the pyrene monomer in the blue and a broad band at higher wavelengths, characteristic of the pyrene excimer emission. At this concentration, intermolecular excimers cannot be formed. The presence of excimer emission upon electronic excitation indicated that the chain-ends of polymer **I** come into contact resulting in the cyclization of the chain.

In Figure 1 , we show the normalized fluorescence spectra (with excitation at 345 nm) of polymer **I** in toluene at −40, 0, and +30 °C. The ratio of excimer to monomer emission intensities depends on the temperature. This change cannot be satisfactorily explained by the variation of the excimer formation rate constant with temperature. Instead, it points to a modification in the cyclization dynamics of the chain. Indeed, at lower temperature, the spectra in the monomer emission region is distorted by new bands that were attributed to the emission of pyrene dimers.[41] This is particularly evident in the spectra at −40 °C.

The variation in the ratio of excimer to monomer emission intensities, collected at 480 and 376 nm, respectively (I_{480}/I_{376}), over the full range of temperatures is shown in Figure 2. Three different regions can be distinguished in this plot, with transitions at around 30 and −30 °C. Similar results were previously obtained for a poly(ϵ-caprolactone) chain, also labeled with pyrene groups at both ends.[42] In that case, the transition taking place at higher temperature was identified as the coil-to-globule transition temperature. Above this temperature, the polymer adopts a coil conformation, while below, it is in a globular state. The transition at lower temperature marked the onset of globule aggregation followed by precipitation.[43]

For polymer **I**, the transition from the coil to the globular state is observed at around 20−30 °C, while the onset of globule aggregation and precipitation appears around −30 °C. We note

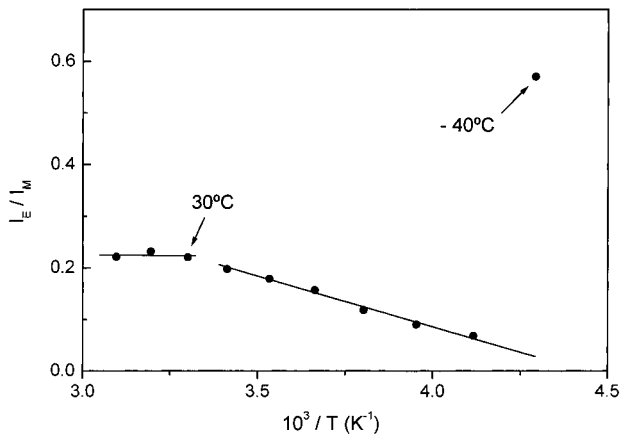

Figure 2. Variation of the pyrene excimer ($\lambda = 480$ nm) to monomer ($\lambda = 376$ nm) fluorescence intensity ratio (I_E/I_M) as a function of temperature for a 10^{-6} M solution of polymer **I** in toluene.

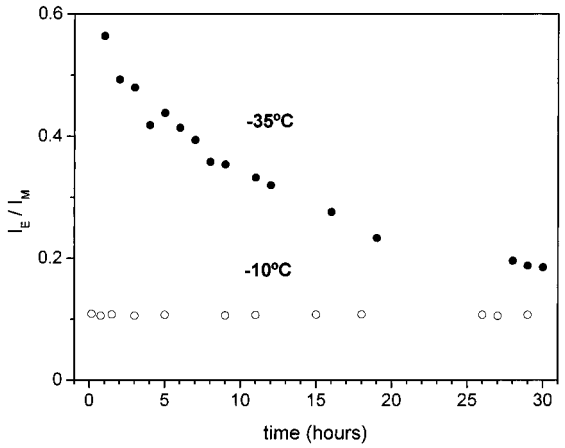

Figure 3. Variation of the pyrene excimer ($\lambda = 480$ nm) to monomer ($\lambda = 376$ nm) fluorescence intensity ratio (I_E/I_M) as a function of delay time after temperature quench for a 10^{-6} M solution of polymer **I** in toluene: (●) −35 and (○) −10 °C.

that the coarse temperature intervals at which the data was collected masks the smooth nature of the coil−globule transition in polymer **I**. Below −30 °C, aggregation of the globules starts, causing the initial increase in I_{480}/I_{376} (more pyrene groups are close enough to produce excimers). The occurrence of aggregation and precipitation also produces a decrease of the I_{480}/I_{376} ratio with the delay time after temperature quenching. Figure 3 shows that, while at −10 °C the I_{480}/I_{376} ratio is constant, at −35 °C it decreases with time (after an initial fast increase, not shown in the figure), due to the depletion of the aggregated polymer from the solution.

The difference in the mobility of the polymer chain, when it is in the coil and in the globule states, can be monitored using the emission of the pyrene groups at the chain ends. The excitation spectra at the monomer and excimer emission wavelengths (Figure 4) are identical when the chain is in the coil state at 30 °C but differ when the polymer attains a globular conformation (0 °C), and eventually aggregates below −30 °C.

In the coil state, the polymer chain is quite loose and the chain ends are far apart, so pyrene dimers are not formed. Instead, upon chain cyclization, dynamic excimers are formed on the encounter of the excited pyrene at one chain end with the pyrene located on the other chain end. Since all the excitation light is absorbed by the pyrene monomer, the excitation spectra recorded at the pyrene monomer and excimer emission regions are identical.

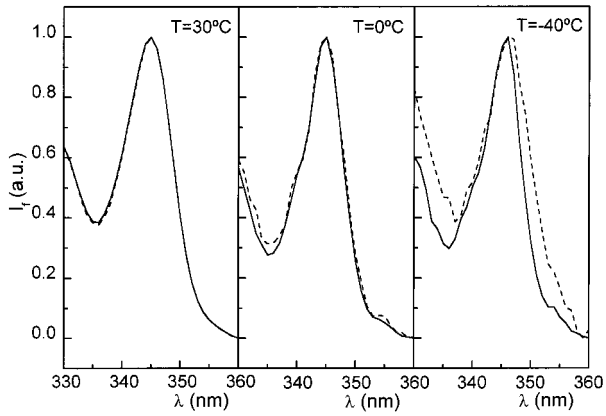

Figure 4. Excitation spectra of a 10^{-6} M solution of polymer **I** in toluene at several quench temperatures. The spectra were recorded immediately after temperature quench at two emission wavelenths: (−) 376 and (- - -) 480 nm.

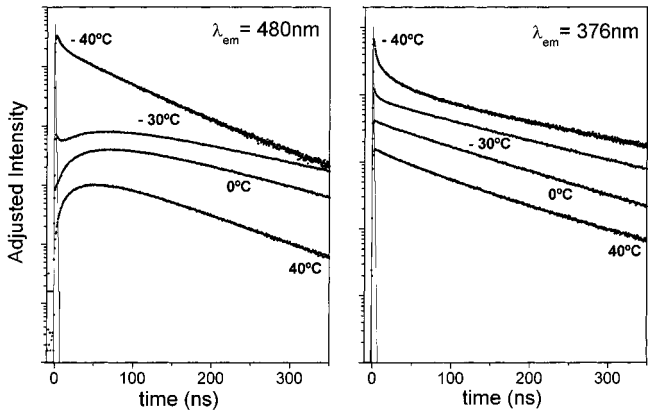

Figure 5. Fluorescence decay curves of pyrene excimer ($\lambda_{em} = 480$ nm) and monomer ($\lambda_{em} = 376$ nm) of a 10^{-6} M solution of polymer **I** in toluene at several temperatures.

Over the globule temperature range, the polymer chain ends are held closer than in the coiled polymer chain. This can lead to preassociation of the pyrene in the ground state, forming dimers that can be directly excited. The excitation light at each wavelength is distributed differently between the pyrene monomer and dimer. As the dimer has its own emission and can convert to the excimer, the excitation spectra recorded at each wavelength reflect the way the emitting species are formed. Therefore, the excitation spectra are different in different regions of the emission spectrum.

Fluorescence Decay Curves. The fluorescence decay curves of a 10^{-6} M solution of polymer **I** in toluene were measured at temperatures from −60 to +60 °C, at the pyrene monomer (376 nm) and excimer (480 nm) emission wavelengths. In Figure 5, we show some of the decay curves obtained. Both the monomer and the excimer decays display remarkable changes as the temperature decreases. For the excimer decays at 480 nm, one passes from a curve characteristic of the formation and decay of a dynamic excimer (40 °C) to a decay with no rise time (−40 °C), typical of a static excimer formed "instantaneously" from the excited dimer. For temperatures between −30 and 30 °C, evidence of both types of excimers was observed. The monomer decays at 376 nm also show changes with temperature that point to a modification on the excited-state kinetics.

In the coil region, from 30 to 60 °C, the excimer decay curves can be fitted with a sum of two exponentials, with the ratio of the preexponential factors close to −1.0, as predicted by Birks for a system with two electronically excited species in equilibrium.[34,35] In Figure 6, we show the excimer decay obtained at +40 °C, fitted with a sum of two exponentials, with rise time $\tau_1 = 34$ ns and decay time $\tau_2 = 90$ ns. The monomer decay curve obtained at the same temperature could only be fitted with a sum of three exponential functions, where the two with lower decay times were identical to the ones obtained in the excimer decay curve analysis (Figure 6) and the one with larger decay time was close to the value obtained for a diluted solution of polymer **II** ($\tau_3 = 175$ ns), which is labeled with pyrene at only one end. The longest decay time in the monomer curve indicates the presence of chains labeled at only one end in polymer **I**.[27,44] From the weight of this longer component to the overall decay law, we determined that approximately 10% of polymer **I** chains are only labeled at one end. This is a usual characteristic of double-end-labeled polymer chains obtained by the process used to label polymer **I**. For temperatures between 30 and 60 °C, polymer **I** is in a coiled conformation (cf. Figure 3), and the excited species are the pyrene monomer and excimer. Over this temperature range, both monomer and excimer decay curves can be fitted with reduced χ^2 close to 1.0 and well distributed residuals and autocorrelation of the residuals.

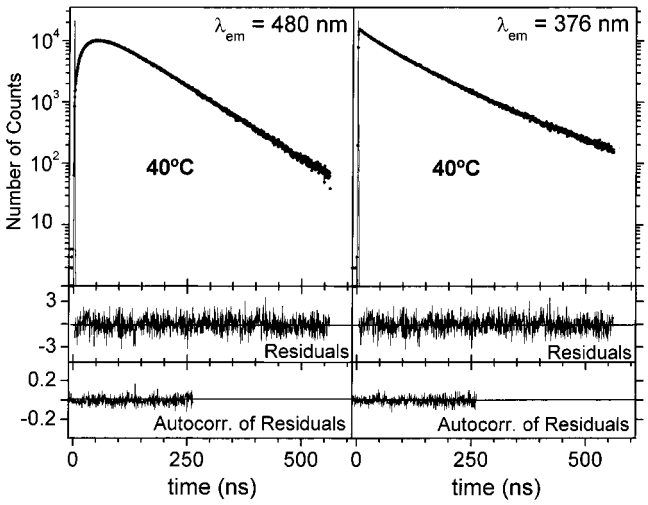

Figure 6. Fluorescence decay curves of pyrene excimer ($\lambda_{em} = 480$ nm) and monomer ($\lambda_{em} = 376$ nm) of a 10^{-6} M solution of polymer **I** in toluene at 40 °C. The excimer decay was fitted with a difference of two exponentials, with lifetimes $\tau_1 = 34$ and 90 ns, preexponential ratio $a_2/a_1 = -0.97$, and $\chi^2 = 1.1$. The monomer decay curve was fitted with a sum of three expenentials with lifetimes $\tau_1 = 34$ ns, $\tau_2 = 90$ ns, and $\tau_M = 175$ ns, preexponential factor ratio $a_2/a_1 = 0.23$, and $\chi^2 = 1.1$.

In the globule region, for temperatures between −30 and 20 °C, the excimer decays could not be fitted with a sum of two exponentials (Figure 7). This is another sign that there are more than two excited-state species involved, confirming the steady-state results where we observed the effect of dimer formation on the I_E/I_M ratio (cf. Figure 2) and a distortion in the fluorescence spectra in the pyrene monomer emission region (cf. Figure 1). The formation of the third species is probably due to the "condensation" of the chain in the globular state that imposes constrains to the polymer chain ends separation. Since the pyrene labeled chain ends are closer, they can associate and form ground-state dimers. The existence of three interconverting excited-state species (monomer, dimer and excimer) implies that the decay curves should be fitted with sums of three exponential functions. This is the case for the excimer decays (emission wavelength 480 nm) obtained at temperatures from 20 to −30 °C. In Figure 7, we show the excimer and monomer decay curves obtained at 0 °C. The excimer decay was fitted with a

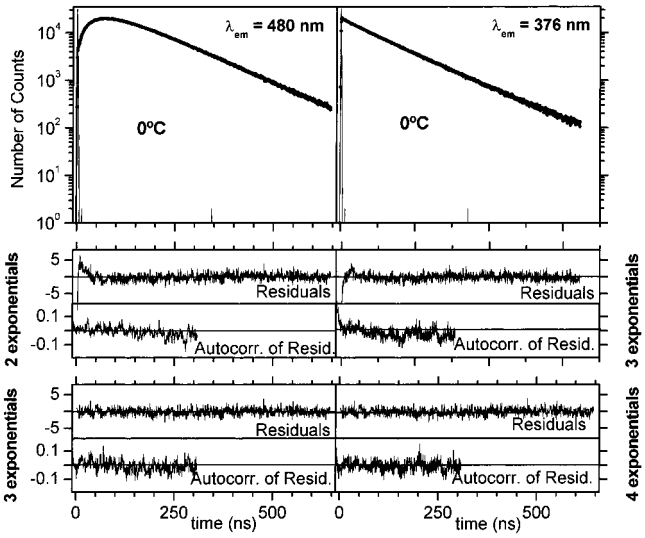

Figure 7. Fluorescence decay curves of pyrene excimer ($\lambda_{em} = 480$ nm) and monomer ($\lambda_{em} = 376$ nm) of the 10^{-6} M solution of polymer **I** in toluene at 0 °C. The excimer decay was fitted with a sum of three exponentials, with lifetimes $\tau_1 = 2$ ns, $\tau_2 = 50$ ns, and $\tau_3 = 117$ ns, preexponential ratios $a_2/a_1 = -25$ and $a_3/a_1 = 26$, and $\chi^2 = 1.1$. The monomer decay curve was fitted with a sum of four expenentials with lifetimes $\tau_1 = 2$ ns, $\tau_2 = 50$ ns, $\tau_3 = 117$ ns, and $\tau_M = 197$ ns, the pre-exponetial ratios $a_2/a_1 = 0.83$ and $a_3/a_1 = 6.7$, and $\chi^2 = 1.0$. The fit of the monomer with a sum of three exponentials and the excimer with a difference of two exponentials is not adequate, as shown by the residuals and the autocorrelation of residuals.

SCHEME 2

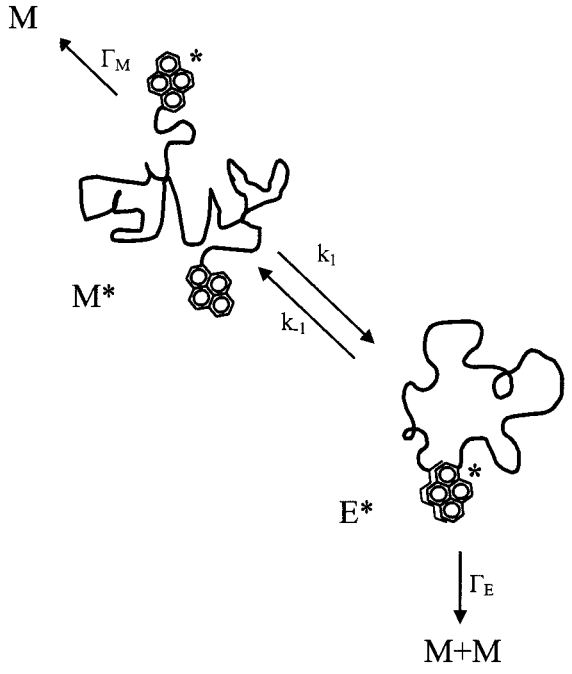

sum of three exponentials, with rise time $\tau_2 = 50$ ns and decay times $\tau_1 = 2$ ns and $\tau_3 = 117$ ns. The monomer decays (emission wavelength 376 nm) in this range of temperatures can only be fitted with a sum of four exponentials, where the term with the longest lifetime accounts for the 10% of one-end-labeled chains in polymer **I**, and the other three lifetimes are close to the ones obtained from the excimer decay.

For temperatures below −30 °C, the decay curves measured at 376 and 480 nm could not be satisfactorily fitted, even with a sum of four exponentials, due to the aggregation of the globules. This causes the variation of fluorescence intensity over long time scales, which was detected as a decrease in the I_{480}/I_{376} ratio (cf. Figure 3).

Kinetic Models. In the previous section, we saw that within the coil region the excimer decay curves could be fitted with a sum of two exponential functions. The monomer decay curves were fitted with a sum of three exponential functions, with the longest decay time very close to the decay time of a diluted solution of polymer **II**. Therefore, in this temperature range, there are only two different excited state species in equilibrium. For a system with two electronically excited species in equilibrium, the kinetics can be described by Scheme 2.[34,35]

The excited species present are the pyrene monomer (M*) and the excimer (E*) formed upon chain cyclization. In the ground state, only the monomer species M exists and is directly excited to give the corresponding excited-state species, M*. The excited pyrene monomer can decay with intrinsic decay constant Γ_M or associate with a ground-state monomer to produce the excimer, E*. This scheme predicts that, after a δ pulse of excitation light, the monomer decays as a sum of two exponential functions and the excimer as a difference of two exponential functions.[34,35] Then, considering that about 10% of PEO chains are monolabeled

$$I_M(t) = a_1^M e^{-\lambda_1 t} + a_2^M e^{-\lambda_2 t} + a_3^M e^{-t/\tau_M} \quad (1)$$

$$I_D(t) = a^D(e^{-\lambda_1 t} - e^{-\lambda_1 t}) \quad (2)$$

where

$$\lambda_i = \frac{(A_x + A_y) + (-1)^i\sqrt{(A_x - A_y)^2 + 4k_1k_{-1}}}{2} \quad (3)$$

$$A_x = \Gamma_M + k_1 \quad (4)$$

$$A_y = \Gamma_E + k_{-1} \quad (5)$$

$$\frac{a_2^M}{a_1^M} = \frac{A_x - \lambda_1}{\lambda_2 - A_x} \quad (6)$$

From the values of the decay parameters λ_1, λ_2, and a_2^M/a_1^M, all the relevant kinetic rate constants can be calculated, once the monomer intrinsic decay constant $\Gamma_M = 1/\tau_M$ is determined from an independent experiment (from the decay of a diluted solution of polymer **II**). The rate constant k_1 corresponds to the cyclization of the coiled chain by formation of the pyrene excimer upon the encounter of the two chain ends, while the rate constant k_{-1} describes the ring opening of the chain.

On the other hand, the excimer and monomer decay curves of polymer **I** in toluene obtained at temperatures from 20 to −30 °C can only be fitted with sums of three exponential functions (four exponential functions in the case of the monomer, corresponding to the last one to the decay of the monolabeled PEO chains in polymer **I**):

$$I_M(t) = a_1^M \exp(-t/\tau_1) + a_2^M \exp(-t/\tau_2) + a_3^M \exp(-t/\tau_3) + a_4^M \exp(-t/\tau_M) \quad (7)$$

$$I_D(t) = a_1^D \exp(-t/\tau_1) + a_2^D \exp(-t/\tau_2) + a_3^D \exp(-t/\tau_3) \quad (8)$$

To describe the kinetics of polymer **I** in toluene at these temperatures, we propose a three-states model. The excited species present are the pyrene monomer (M*), a dimer (D*),

and the excimer (E*). The dimer and excimer correspond to different conformations of the associated state of the two chain-end pyrene moieties. The ground-state species M and D are in equilibrium and upon electronic excitation can give the corresponding excited-state species, M* and D*. The ground state of the pyrene excimer is dissociative, and therefore E*, cannot be produced by direct excitation. The excimer can only be produced either from the encounter of an excited monomer M* with a ground-state monomer M or from rearrangement of the excited dimer D*. The three excited species can lose the excitation energy with intrinsic decay constants Γ_M, Γ_D, and Γ_E.

The general kinetic scheme for a system with three excited interconverting species[41,45] can be simplified if we consider that, once formed, the excimer will not produce excited dimer ($k_{-3} = 0$) and can only decay to ground-state monomers with intrinsic lifetime Γ_E or dissociate to give M and M*, with rate constant k_{-1}. This assumption is justified because the excimer corresponds to a more favorable pyrene conformation compared to the dimer. Also, it was later verified that letting the value of k_{-3} change freely during the fitting procedure leads to k_{-3} values close to zero with no influence on the value of the remaining kinetic constants or the quality of the fit. The resulting kinetic Scheme 3 can be solved using standard procedures[45] to give the expressions of three decay rate constants ($\lambda_i = -1/\tau_i$, $i = 1, 2, 3$) and the ratios of monomer and excimer preexponential parameters in eqs 7 and 8.

The decay constants are given by

$$\begin{cases} \lambda_1 = -\beta(2\cos\gamma) - \dfrac{a_2}{3} \\ \lambda_2 = -\beta(\cos\gamma + \sqrt{3}\sin\gamma) - \dfrac{a_2}{3} \\ \lambda_3 = -\beta(\cos\gamma - \sqrt{3}\sin\gamma) - \dfrac{a_2}{3} \end{cases} \tag{9}$$

with

$$\begin{cases} \gamma = \dfrac{1}{3}\mathrm{arctg}\left(\dfrac{\sqrt{|\Delta|}}{r}\right) \\ \beta = (r^2 + |\Delta|)^{1/6} \end{cases} \tag{10}$$

$$\begin{cases} \Delta = r^2 + q^3 \\ r = \dfrac{-3a_0 + a_1a_2}{6} - \dfrac{{a_2}^3}{27} \\ q = \dfrac{a_1}{3} - \dfrac{{a_2}^2}{9} \end{cases} \tag{11}$$

$$\begin{cases} a_0 = ABC - k_2k_{-2}B - k_1k_{-1}C - k_{-1}k_2k_3 \\ a_1 = AB + BC + CA - k_1k_{-1} - k_3k_{-3} \\ a_2 = A + B + C \end{cases} \tag{12}$$

$$\begin{cases} A = \Gamma_M + k_1 + k_2 \\ B = \Gamma_E + k_{-1} \\ C = \Gamma_D + k_{-2} + k_3 \end{cases} \tag{13}$$

and the ratios of monomer and excimer preexponential parameters are given by

$$\begin{cases} \dfrac{a_1^M}{a_2^M} = \dfrac{\alpha_1 c_{11}^0}{\alpha_2 c_{21}^0} \\ \dfrac{a_1^M}{a_3^M} = \dfrac{\alpha_1 c_{11}^0}{\alpha_3 c_{31}^0} \\ \dfrac{a_1^D}{a_2^D} = \dfrac{\alpha_1 (c_{12}^0 + c_{13}^0)}{\alpha_2 (c_{22}^0 + c_{23}^0)} \\ \dfrac{a_1^D}{a_3^D} = \dfrac{\alpha_1 (c_{12}^0 + c_{13}^0)}{\alpha_3 (c_{32}^0 + c_{33}^0)} \end{cases} \tag{14}$$

with

$$\begin{cases} c_{i1}^0 = k_{-2}(B + \lambda_i) + k_{-1}k_3 \\ c_{i2}^0 = k_3(A + \lambda_i) + k_1k_{-2} \\ c_{i3}^0 = (A + \lambda_i)(B + \lambda_i) - k_1k_{-1} \end{cases} \tag{15}$$

$$\begin{cases} \alpha_1 = \dfrac{[M]_0 - c_{31}^0\alpha_3 - c_{21}^0\alpha_2}{c_{11}^0} \\ \alpha_2 = -\dfrac{\alpha_3\Theta_2 + c_{12}^0[M]_0 - c_{11}^0[D]_0}{\Theta_3} \\ \alpha_3 = \dfrac{(c_{11}^0[D]_0 - c_{12}^0[M]_0)\Theta_4 - c_{13}^0[M]_0\Theta_3}{\Theta_1\Theta_3 + \Theta_2\Theta_4} \end{cases} \tag{16}$$

$$\begin{cases} \Theta_1 = c_{11}^0c_{22}^0 - c_{12}^0c_{21}^0 \\ \Theta_2 = c_{13}^0c_{21}^0 - c_{11}^0c_{23}^0 \\ \Theta_3 = c_{11}^0c_{33}^0 - c_{13}^0c_{31}^0 \\ \Theta_4 = c_{11}^0c_{32}^0 - c_{12}^0c_{31}^0 \end{cases} \tag{17}$$

The monomer decay rate constant Γ_M can be obtained independently (using a diluted solution of polymer **II**), and so we are left with eight kinetic parameters to be determined: the chain cyclization rate constants k_1 and k_2 for the formation of excimer and dimer; the ring-opening rate constants k_{-1} and k_{-2} corresponding to the dissociation of the excimer and the dimer; the rate constant for conversion of dimer to excimer k_3; the intrinsic decay rate constants of the excimer Γ_E and the dimer Γ_D; and a parameter $[M^*]^0/[D^*]^0$ relating the amounts of excited monomer and dimer obtained immediately after excitation.

Kinetic Analysis. For the decays in the coil region, from 30 to 60 °C, the values of the decay parameters λ_1, λ_2 and the ratio a_1^M/a_2^M in eqs 1 and 2 were used to calculate all the relevant kinetic rate constants. The $\Gamma_M = 1/\tau_M$ values were obtained from the monoexponential decay curves of dilute solutions (10^{-6} M) of polymer **II**, labeled with 1-pyrenyl group at only one chain end (Table 1).

We fitted the excimer decay curves with a sum of two exponentials and the monomer decay curves with a sum of three exponentials, with the longest decay constant close to Γ_M and the other two close to the values obtained from the fitting of the excimer decay. The decay rate constants obtained from the excimer decay are recovered with higher precision since the decay is a difference of two exponentials.[46] To obtain the most reliable values of the decay rate constants, we performed constrained fittings of the monomer decay curves. The longest decay constant at each temperature was fixed to the value obtained from the monoexponential decay curve of polymer **II** solution, and the other two decay constants were constrained to the values obtained for the excimer decay curve analysis. Even in these extreme conditions, where only the preexponential

SCHEME 3

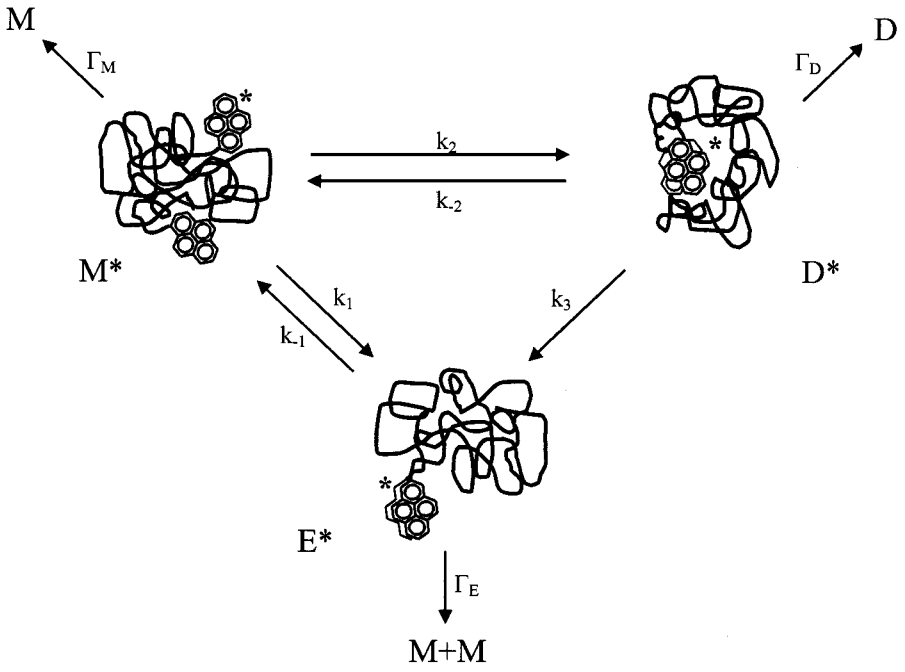

TABLE 1: Monomer Intrinsic Lifetimes Determined from a Diluted Solution of Polymer II

T/°C	−30	−20	−10	0	10	20	30	40	50	60
τ_M/ns	194	195	196	197	196	194	183	180	176	172

factors were fitted, we obtained good results, with reduced χ^2 close to 1.0 and well-distributed weighted residuals and autocorrelation of the residuals.

In the globule region, from −30 to +20 °C, the excimer decay curves were fitted by a sum of three exponentials, according to eq 8. The monomer decay curves were fitted with a sum of four exponential functions, the longest decay constant being close to Γ_M and the remaining decay constants close to the values obtained from the fitting of the excimer decay. As for the coil region, we reanalyzed the monomer decay curves, constraining their lifetimes in order to obtain the best values of the rate constants. Again, the longest decay constant was fixed to the value obtained from the monoexponential decay curves of polymer **II** solutions (Table 1), and the remaining decay constants were constrained to the values obtained for the excimer decay curve. In all the fittings, we got reduced χ^2 close to 1.0 and well-distributed weighted residuals and autocorrelation of the residuals.

For the globule region, the calculation of the kinetic rate parameters is more complex than that for the coil region. In this case, eqs 7−17 cannot be inverted in order to obtain the kinetic rate constants directly. Therefore, we had to use a grid mapping method to obtain the most probable values of the kinetic rate parameters from the fitted parameters.[47] First, we have done a coarse grid mapping of the model parameter space in order to identify the region of minimum reduced χ^2. Over this region, the search was refined dividing the probable range of values for each parameter p_j in a number n_j of equal increments. The parameter space was thus divided in $\prod_j n_j$ hypercubes, at which vertexes the χ^2 was evaluated, to define a narrower region for the χ^2 minimum. This procedure was repeated until the change in the results was lower than the desired tolerance (in the present case 1%).

For each temperature, we obtained two decays, at excitation wavelengths of 376 and 480 nm. From the analysis of these two decays, we can obtain seven independent parameters: three decay rate constants λ_1, λ_2, and λ_3; two ratios of monomer preexponential factors a_1^M/a_2^M and a_1^M/a_3^M; and two ratios of excimer preexponential factors a_1^E/a_2^E and a_1^E/a_3^E. Therefore, we can only determine seven kinetic parameters for the present system, and since we have nine unknown kinetic parameters in the model, we must obtain independent information on the system. First, we have already seen that the monomer intrinsic lifetime can be determined independently from the decay of a diluted solution of polymer **II** (Table 1).

As a first approach, we have considered that excimer and dimer dissociate with the same rate constant $k_{-1} = k_{-2}$ and obtained the remaining rate constants. In this way, we verified that the obtained excimer intrinsic decay constant Γ_E is almost insensitive to the temperature and its value coincides with the values accepted in the literature.[29,45,48,49] We then fixed the $\Gamma_E = 1/\tau_E$ value to its average value ($\tau_E = 51$ ns) obtained in this approach. With this, we decreased one degree of freedom in the system, and therefore, we can consider that the excimer and dimer dissociation rate constants are independent, i.e., that the excimer and dimer binding energies are not necessary equal.

Therefore, the rate constants to be obtained in the fitting procedure are: the cyclization rate constants for the formation of excimer and dimer, k_1 and k_2; the ring-opening rate constants of the polymer chain with dissociation of dimer and excimer, k_{-1} and k_{-2}; the rate constant for dimer rearrangement with conversion to the excimer, k_3; the intrinsic decay constant of the dimer, Γ_D; and the parameter $[M^*]^0/[D^*]^0$ relating the amounts of excited monomer and dimer obtained directly upon excitation. Within experimental error, the amount of excited dimer initially produced by excitation at the wavelength of 330 nm was found to be about 50 ± 10 times smaller than the amount of excited monomer produced.

In Figure 8, we show the variation of the intrinsic decay constants $\Gamma_M = 1/\tau_M$, $\Gamma_E = 1/\tau_E$, and $\Gamma_D = 1/\tau_D$ (τ_M, τ_E, and τ_D being the intrinsic lifetimes of the monomer, excimer, and dimer species, respectively) with temperature, for the coil and globule states, between −30 and +60 °C. The excimer intrinsic lifetime was held fixed at $\tau_E = 51$ ns below 30 °C. The intrinsic decay

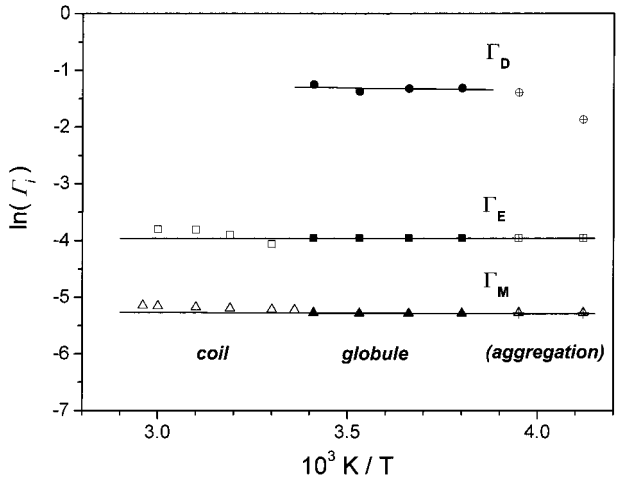

Figure 8. Variation of the reciprocal of the intrinsic lifetimes of pyrene dimer (Γ_D), excimer (Γ_E) and monomer (Γ_M) vs $1/T$ in the coil and globule temperature regions.

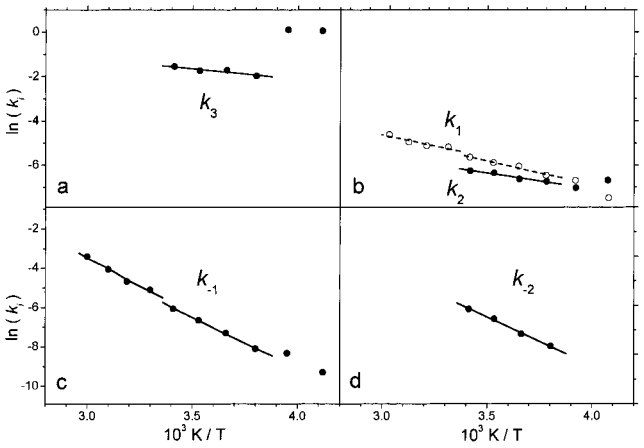

Figure 9. Arrhenius plots of the monomer−excimer (k_1), monomer−dimer (k_2) dimer−excimer (k_3), and the reverse dimer−monomer (k_{-2}) and excimer−monomer (k_{-1}) rate constants.

constants of the other two excited species show a limited dependence on the temperature over the full range of temperatures studied, with average values of the intrinsic lifetimes being $\tau_D = 4$ ns and $\tau_M = 188$ ns. From the values of Γ_D in Figure 8, we can also notice that for the two lowest temperatures studied, the three states model fails to give consistent results. We attribute this behavior to the aggregation and precipitation of the polymer globules that begins around −30 °C (cf. Figure 2).

In Figure 9, we show the Arrhenius plots of the kinetic rate constants for interconversion between the three excited species. Also, here it is evident that the three-state model does not describe the data close to the onset of aggregation and precipitation of the polymer globules at −30 °C. The rate of conversion of the excited dimer to excimer, k_3, is relatively high compared to the rates of monomer/dimer and monomer/excimer related processes (Figure 9 a), suggesting that the conversion of excited dimer to excimer is a favorable process. This was expected since the process only involves the reorientation of the pyrene groups through a local rearrangement of the chain ends.

The values of the rate constants for cyclization of polymer **I** through the formation of the excimer, k_1, are only slightly higher than those for the formation of dimer, k_2 (Figure 9 b). We observe that the values of k_1 have a continuous variation with temperature across the coil to globule transition temperature

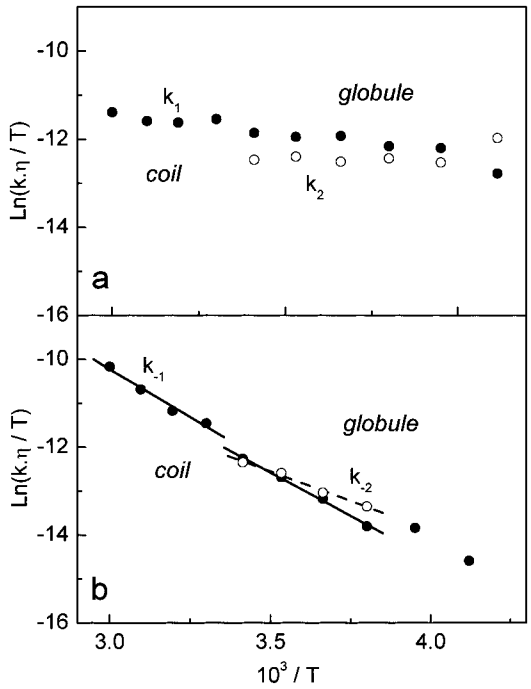

Figure 10. Plots of the monomer−excimer (k_1) and monomer−dimer (k_2) and the reverse dimer−monomer (k_{-2}) and excimer−monomer (k_{-1}) rate constants multiplied by η/T (to correct for the influence of the diffusion coefficient).

region. On one hand, this shows that the two different models used to analyze our data in the coil and globule regions give consistent results. On the other hand, we can conclude that the kinetics of excimer formation itself is not affected by this transition. The major effect of the formation of globules is the appearance of dimers. The formation of this species is due to the constrains imposed by the chain in the more compact globule conformation. However, for the globules in which the chain-ends are less constrained (for example, because of being segregated to the surface of the globule), excimer formation is still possible and proceeds as in the coiled chain.

The kinetic rate constants for the ring-opening reaction (separation of the polymer chain-ends) with dissociation of the excimer k_{-1} and the dimer k_{-2} are very similar (Figure 9c,d). Again, the values of k_{-1} show a continuous variation across the coil to globule transition temperature.

To compare the variations of the different kinetic rate constants with temperature, they must be corrected for their dependence on the diffusion coefficients.[25] Effects such as excluded volume, chain stiffness, and hydrodynamic properties of the polymer do not change significantly with temperature for low molecular weight polymers.[4,50]

The cyclization rate constants are proportional to the translational diffusion coefficient of the chain.[25] As the diffusion coefficient depends on T/η, where η is the viscosity of the solvent, its influence on the cyclization rate constants can be removed multiplying the rate constants by η/T. The $k_1\ \eta/T$ and $k_2\ k\ \eta/T$ values presented in Figure 10a are essentially constant over the entire range of temperatures. These two processes correspond to the cyclization of the polymer chain via excimer and dimer formation, respectively. As the dependence of the rate constants on temperature is almost completely accommodated by the temperature dependence of the diffusion coefficient, we conclude that both processes are diffusion-controlled. This suggests that even in the globular state the chain ends have some mobility, pointing to the existence of swollen

TABLE 2: Values Obtained for the Enthalpy of Cyclization ΔH in the Coil and Globule (excimer and dimer formation) Chain Conformations of Polymer I[a]

	ΔH (kJ/mol) (ring-opening reaction)	$-\Delta H°$ (kJ/mol) (cyclization equilibrium)	$\Delta S°$ (J/K mol) (cyclization equilibrium)
coil	36 ± 4	32 ± 1	-107 ± 4
globule			
excimer	33 ± 1	27 ± 1	-89 ± 5
dimer	22 ± 2	22.0 ± 0.4	-76 ± 1

[a] The values where obtained from the Arrhenius plots of the ring-opening rate constants k_{-1} and k_{-2}, corrected for the temperature effects on chain dynamics using the term η/T (eq 18). Also shown are the values of the enthalpy $\Delta H°$ and entropy $\Delta S°$ of cyclization obtained from the van t′Hoff plots of the equilibrium cyclization constants (eq 19).

globules that incorporate a large percentage of solvent.[36] Loose, solvent swollen globules are expected for small flexible chains such as polymer **I**, with $M_w < M_e$ and therefore no entanglements.

For the ring-opening process, the correction of k_{-1} and k_{-2} for their dependence on the diffusion coefficient does not explain the dependence of this process on temperature (Figure 10b).

The ring-opening reaction involves excimer or dimer dissociation. So, before the two chain ends can diffuse apart, disruption of the excimer or dimer binding energy has to occur. For excimer dissociation between free chromophores the ring-opening rate constant can be expressed as[51,52]

$$k_{open} \propto D \exp\left(-\frac{\Delta H}{RT}\right) \qquad k_{open} = k_{-1}, k_{-2} \qquad (18)$$

where D is the mutual diffusion coefficient and ΔH is the excimer or dimer binding energy. In our case, the chromophores are attached to the ends of a polymer chain, and the process is necessarily more complex, reflecting all aspects of the polymer−solvent interaction that operate on the conformation and dynamics of the chain. Table 2 shows the excimer and dimer binding energies calculated from the Arrhenius plots of $k_{-1}\ \eta/T$ and $k_{-2}\ k\ \eta/T$ (Figure 10b), respectively. In the globule region, the value obtained for the excimer binding energy $\Delta H = 33 \pm 1$ kJ mol^{-1} is higher than the value for the dimer binding energy $\Delta H = 22 \pm 2$ kJ mol^{-1}, confirming the constrained conformation of the pyrene groups in the formation of a dimer species. For the coiled chain, we calculated that the excimer binding energy $\Delta H = 36 \pm 4$ kJ mol^{-1} is only slightly higher than that for the chain in the globule conformation, the difference not being relevant to be attributed to a decrease in the polymer chain-end mobility in the globular state. These values are in very good agreement with the values accepted for the intermolecular excimer binding energy of free chromophores ($\Delta H \approx 36-40$ kJ mol^{-1}),[29,45,48] indicating that eq 18 describes well the intramolecular excimer dissociation. Nevertheless, any effect of temperature on polymer dynamics that is not accommodated by the η/T correction and the variation of the excluded volume can make a contribution to ΔH.

In Figure 11, we show the van t'Hoff plots of the cyclization equilibrium constants, calculated as $K_1 = k_1/k_{-1}$ (monomer−excimer) and $K_2 = k_2/k_{-2}$ (monomer−dimer), for polymer **I** in the coil and globule states. The most striking point in the plot of K_1 is that its values over the coil-to-globule transition are in very good agreement. For the lowest two temperatures, the plot is nonlinear because the polymer is probably aggregated (cf. Figure 2). For the same reason, it was not possible to calculate the K_2 value for these two temperatures.

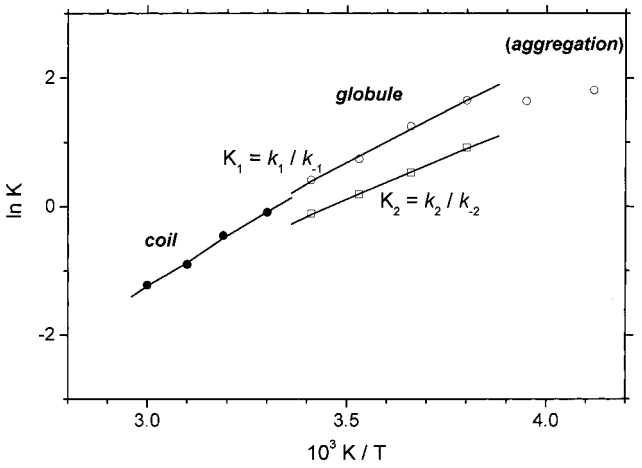

Figure 11. van t'Hoff plots of the monomer−excimer (K_1) and monomer−dimer (K_2) equilibrium constants in the coil and globule temperature ranges.

The slopes of the K_1 and K_2 van t'Hoff plots are identical (Figure 11), indicating that the excimer and excited dimer species behave similarly when the polymer is in the globular state. The cyclization equilibrium constants are given by

$$K_i = \exp\left(\frac{\Delta S_i^0}{R}\right) \exp\left(\frac{-\Delta H_i^0}{RT}\right) \qquad i = 1, 2 \qquad (19)$$

where ΔH_i^0 and ΔS_i^0 are the enthalpy and entropy of cyclization, for excimer ($i = 1$) and dimer formation ($i = 2$). Table 2 shows the $\Delta H°$ and $\Delta S°$ values obtained from the fitting of the experimental cyclization equilibrium constants to eq 19. The enthalpy of pyrene excimer formation absolute value is higher in the coil (32 ± 1 kJ mol^{-1}) than in the globule (27 ± 1 kJ mol^{-1}), in accordance with the correspondent binding energies. The difference between the enthalpy and the binding energy of the excimer is due to the variation in energy between the cyclized and noncyclized polymer conformations in equilibrium. These conformation changes do not contribute to the excimer dissociation enthalpy, where only the process of separation of the two pyrenyl groups is accounted for. Similar trends were observed for the cyclization of polystyrene in several solvents.[30] The binding and the enthalpy for the dimer in the globule are similar. This means that the enthalpy of polymer conformation for the cyclyzed and noncyclized chains in equilibrium is equal. This can probably result from the fact that the dimer is only formed for those polymer conformations that force the association of the two pyrenes. For these conformations, the dissociation of the dimer does not induce significant changes on the enthalpy of the polymer conformation. The lowest absolute value for pyrene dimer formation enthalpy (22 ± 2 kJ mol^{-1}) compared to the excimer (27 ± 1 kJ mol^{-1}) in the globular state is due to the less favorable configuration of the two pyrene moieties in the dimer than in the excimer.

The entropy change $\Delta S°$ is negative for all processes because cyclization increases the ordering of the polymer chain, decreasing the entropy. The change in $\Delta S°$ follows the same trend as $-\Delta H°$, with the most important entropy loss corresponding to the formation of the most stable conformation. The highest entropy loss is detected for the formation of excimer in a coiled chain ($\Delta S° = -107 \pm 4$ J K^{-1} mol^{-1}), closely followed by the constrained formation of the excimer by a chain in the globular state ($\Delta S° = -89 \pm 5$ J K^{-1} mol^{-1}) and, finally, the formation of an excited dimer ($\Delta S° = -76 \pm 1$ J K^{-1} mol^{-1}).

Conclusions

The stable globule state of isolated polymer chains is very difficult to observed because of the very low concentrations that are necessary to avoid the aggregation and precipitation of the globules. At such low concentrations, most techniques (e.g., light scatering) are not sensitive enough. In this work, we used fluorescence to characterize the coil−globule transition of isolated PEO chains in toluene.

The fluorescence spectra and decay curves of a poly(ethylene oxide) chain with both ends labeled with pyrene (polymer **I**) in toluene show significant variations around 30 °C. Above 30 °C, the pyrene fluorescence spectra show two bands characteristic of the pyrene monomer and excimer emissions. Below this temperature, new bands superposed to the pyrene monomer emission were detected in the fluorescence spectra. These bands were attributed to the emission of a pyrene dimer also present in the ground-state. The variation of the pyrene excimer to monomer fluorescence intensity ratio with temperature shows a transition around 30 °C. According to the steady-state results, the decay curves can be explained by a two-state (excited pyrene monomer and excimer) model above and a three-state (excited pyrene monomer, dimer, and excimer) below 20 °C. This results point to a broad coil-to-globule transition taking place at around 30 °C. We could expect a broad transition since polymer **I** is flexible and relatively small ($M_w < M_e$), presenting no entanglements. However, the 10 °C temperature intervals of the fluorescence measurements did not allow the precise determination of the transition broadness.

The activation energies for both pyrene excimer and dimer are similar to the toluene viscous flow activation energies, showing that these processes are diffusion-controlled. The pyrene excimer binding energy in the coil is higher than that in the globule according to a less stable pyrene excimer conformation in the globule imposed by the polymer "condensed" conformation. The binding energy of pyrene dimer is lower than that the excimer binding energy, which explains the irreversibility of the excited dimer to excimer conversion. The enthalpy of pyrene excimer formation in both the coil and the globule are lower than the corresponding binding energies reflecting the distinction between the cyclized and noncyclized polymer conformations.

Acknowledgment. We acknowledge the financial support from FCT through project PRAXIS/P/QUI/14057/1998. S. Piçarra acknowledges the grant GGPXXI/BD/2979/96. We thank Dr. A. Fedorov for the setting of the laser time-resolved fluorescence equipment.

References and Notes

(1) Doniach, S.; Garel, T.; Orland, H. *J. Chem. Phys.* **1996**, *105*, 1601.
(2) Chan, H. S.; Dill, K. A. *Phys. Today* **1993**, 24.
(3) Takahashi, M.; Yoshikawa, K.; Vasilevskaya, V. V.; Khokhlov, A. R. *J. Phys. Chem. B* **1997**, *101*, 9396.
(4) Grosberg, A.; Yu.; Khokhlov, A. R. *Statistical Physics of Macromolecules*; AIP Press: New York, 1994.
(5) Doye, J. P. K.; Sear, R. P.; Frenkel, D. *J. Chem. Phys.* **1998**, *108*, 2134.
(6) Flory, P. J. *J. Chem. Phys.* **1949**, *17*, 303.
(7) Raos, G.; Allegra, G. *J. Chem. Phys.* **1997**, *107*, 6479.
(8) Hu, W. *J. Chem. Phys.* **1998**, *109*, 3686.
(9) Monnerie, L. In *Photophysical and Photochemical Tools in Polymer Science*; Winnik, M. A., Ed.; D. Reidel: Dordrecht, The Netherlands, 1985.
(10) Winnik, M. A. *Acc. Chem. Res.* **1985**, *18*, 73.
(11) Winnik, M. A. In *Photophysical and Photochemical Tools in Polymer* Science; NATO ASI Series; Winnik, M. A. Ed.; Reidel: Dordrecht, The Netherlands, 1986; Vol. 182.
(12) Winnik, M. A.; Redpath, A. E. C.; Paton, K.; Danhelka, J. *Polymer* **1984**, *25*, 91.
(13) Morawetz, H. *J. Lumin.* **1989**, *43*, 59.
(14) Horinaka, J.; Ito, S.; Yamamoto, M.; Tsujii, Y.; Matsuda, T. *Macromolecules* **1999**, *32*, 2270.
(15) Kitamura, S. Yunokawa, H.; Kuge, T. *Polym. J.* **1982**, *14*, 85.
(16) Horinaka, J.; Maruta, M.; Ito, S.; Yamamoto, M. *Macromolecules* **1999**, *32*, 1134.
(17) Förster, Th. *Ann. Phys.* **1948**, *2*, 55.
(18) Liu, G.; Guillet, J. E. *Macromolecules* **1990**, *23*, 1393.
(19) Liu, G.; Guillet, J. E.; Al-Takrity, E. T. B.; Jenkins, A. D.; Walton, D. R. M. *Macromolecules* **1991**, *24*, 68.
(20) Dos Remedios, C. G.; Moens, P. D. *J. Struct. Biol.* **1995**, *115*, 175.
(21) Wu. P.; Brand, L. *Anal. Biochem.* **1994**, *218*, 1.
(22) Haas, E.; Katchalski-Katzir, E.; Seinberg, I. Z. *Biopolymers* **1978**, *17*, 11.
(23) Lakowicz, J. R.; Kusba, J.; Wiczk, W.; Gryczynski, I.; Johnson, M. L. *Chem. Phys. Lett.* **1990**, *173*, 319.
(24) Cuniberti, C.; Perico, A. *Eur. Polym. J.* **1977**, *13*, 369.
(25) Cuniberti, C.; Perico, A. *Prog. Polym. Sci.* **1984**, *10*, 271.
(26) Winnik, M. A.; Redpath, A. E. C. *J. Am. Chem. Soc.* **1980**, *102*, 6869.
(27) Martinho, J. M. G.; Martinho, M. H.; Winnik, M. A.; Beinert, G. *Makromol. Chem. Suppl.* **1985**, *15*, 113.
(28) Martinho, J. M. G. Winnik, M. A. *Macromolecules* **1986**, *19*, 2281.
(29) Martinho, J. M. G.; Reis e Sousa, A. T.; Winnik, M. A. *Macromolecules* **1993**, *26*, 4484.
(30) Reis e Sousa, A. T.; Castanheira, E. M. S.; Fedorov, A.; Martinho, J. M. G. *J. Phys. Chem. A* **1998**, *102*, 6406.
(31) Redpath, A. E. C.; Winnik, M. A. *J. Am. Chem. Soc.* **1982**, *104*, 5604.
(32) Martinho, J. M. G.; Castanheira, E. M. S.; Reis e Sousa, A. T.; Saghbini, S.; André, J. C.; Winnik, M. A. *Macromolecules* **1995**, *28*, 1167.
(33) Reis e Sousa, A. T.; Castanheira, E. M. S.; Martinho, J. M. G.; Saghbini, S.; Baros, F.; André, J. C.; Winnik, M. A. *Chem. Phys. Lett.* **1993**, *213*, 333.
(34) Birks, J. B. *Photophysics of Aromatic Molecules*; Wiley-Interscience: London, 1970.
(35) Birks, J. B. *Rep. Prog. Phys.* **1975**, *38*, 903.
(36) Yu, J.; Wang, Z.; Chu, B. *Macromolecules* **1992**, *25*, 1618.
(37) Marquardt, D. W. *J. Soc. Ind. Appl. Math.* **1963**, *11*, 431.
(38) Cheung, S.-T.; Winnik, M. A.; Redpath, E. C. *Makromol. Chem.* **1982**, *183*, 1815.
(39) Winnik, M. A.; Redpath, A. E. C.; Paton, K.; Danhelka *J. Polymer* **1984**, *1251*, 91.
(40) Ghiggino, K. P.; Snare, M. J.; Thistlethwaite, P. J. *Eur. Polym. J.* **1985**, *21*, 265.
(41) Winnik, F. M. *Chem. Rev.* **1993**, *93*, 587.
(42) Piçarra, S.; Gomes, P. T.; Martinho, J. M. G. *Macromolecules* **2000**, *33*, 3947.
(43) Piçarra, S.; Martinho, J. M. G. *Macromolecules* **2001**, *34*, 53.
(44) Boileau, S.; Méchin, F.; Martinho, J. M. G.; Winnik, M. A. *Macromolecules* **1989**, *22*, 215.
(45) Farinha, J. P. S.; Martinho, J. M. G.; Xu, H.; Winnik, M. A.; Quirk, R. P. *J. Polym. Sci.: Polym. Phys.* **1994**, *32*, 1635.
(46) Farinha, J. P. S.; Martinho, J. M. G.; Pogliani, L. *J. Math. Chem.* **1997**, *21*, 131.
(47) Bevington, P. R. *Data Reduction and Error Analysis in the Physical Sciences*; MaGraw-Hill: New York, 1969.
(48) Martinho, J. M. G.; Farinha, J. P. S.; Berberan-Santos, M. N.; Duhamel, J.; Winnik, M. A. *J. Chem. Phys.* **1992**, *96*, 8143.
(49) Berberan-Santos, M. N.; Farinha, J. P. S.; Martinho, J. M. G.; Duhamel, J.; Winnik, M. A. *Chem. Phys. Lett.* **1992**, *189*, 328.
(50) Doi, M.; Edwards, S. F. *The Theory of Polymer Dynamics*; Oxford University Press: New York, 1988.